Wave propagation in compact, thin-walled, layered, and heterogeneous structures using variable kinematics finite elements

Wave propagation in compact, thin-walled, layered, and heterogeneous structures using variable kinematics finite elements

M. Petrolo*[1], I. Kaleel†[1], G. De Pietro‡[1,2], and E. Carrera§[1]

[1]MUL^2 Group, Department of Mechanical and Aerospace Engineering, Politecnico di Torino , Turin, Italy
[2]Materials Research and Technology Department, Luxembourg Institute of Science and Technology , Esch-sur-Alzette, Luxembourg

Revised version of UCME-2017-0038

Author for correspondence:
Erasmo Carrera, Professor of Aerospace Structures and Aeroelasticity
MUL^2 Group, Department of Mechanical and Aerospace Engineering,
Politecnico di Torino,
Corso Duca degli Abruzzi 24,
10129 Torino, Italy,
tel: +39 011 090 6836,
fax: +39 011 090 6899,
e-mail: erasmo.carrera@polito.it

*Assistant Professor, marco.petrolo@polito.it
†Ph.D. Student, ibrahim.kaleel@polito.it
‡Ph.D. Student, gabriele.depietro@list.lu
§Professor of Aerospace Structures and Aeroelasticity, erasmo.carrera@polito.it

Abstract

The paper investigates wave propagation characteristics for a class of structures using higher-order one-dimensional (1D) models. 1D models are based on the Carrera Unified Formulation (CUF), a hierarchical formulation which provides a framework to obtain refined structural theories via a variable kinematics description. Theories are formulated by employing arbitrary expansions of the primary unknowns over the beam cross-section. Two classes of beam models are employed in the current work, namely Taylor Expansion (TE) and Lagrange Expansion (LE) models. Using the principle of virtual work and finite element method, the governing equations are formulated. The direct time integration of equation of motion is carried through an implicit scheme based on the Newmark method and a dissipative explicit method based on the Tchamwa-Wielgosz scheme. The framework is validated by comparing the response for the stress wave propagation in an isotropic beam to an analytical solution available in the literature. The capabilities of the proposed model are demonstrated by presenting results for wave propagation analysis of a sandwich beam and a layered annular cylinder structure. The ability of CUF models to detect 3D-like behavior with a reduced computational overhead is highlighted.

Keywords: Wave Propagation, Travelling Loads, Composites, Carrera Unified Formulation, 1D Models, FEM.

1 Introduction

Advanced structural systems made of composite and sandwich materials are gaining popularity for aerospace and automobile applications under dynamic loading conditions. These structures are often slender in nature such as aircraft wings and fuselage, rockets and launchers, therefore can be modeled as 1D structures. Such structures are often subjected to high-frequency loads, which leads to importance for understanding the wave characteristics of such systems.

Euler and Bernoulli developed the classical beam theory, which simplified the linear theory of elasticity for calculating the beam deflection and load-carrying characteristics for 1D structures [1]. Timoshenko introduced the shear and rotary inertia into Euler-Bernoulli beam theory (EBBT) with an assumption of constant shear strain across the cross-section [2]. Timoshenko Beam Theory (TBT) significantly increased the range of applicability of the classical 1D models. However, practical engineering problems are often accompanied by geometric variations and material heterogeneity where classical beam theories can lead to incorrect responses. Hereafter, some of the most important contributions are discussed with particular attention paid to dynamics responses and wave propagation problems. A more comprehensive review of beam models can be found in [3].

Over the last couple of decades, much effort has been devoted towards improving the classical and refined beam models [4–7]. Bank et al. reported a beam theory based on TBT for the dynamic response of thin-walled composite beams [4, 8]. The model accounted for material heterogeneity of composites by providing appropriate constants for the TBT equations. Murakami et al. proposed a 1D model for elastic wave propagation for heterogeneous beams by making a dynamic extension to Reissner's mixed variational equation [5]. The model was able to capture stress concentrations with great accuracy under dynamic loading conditions. Even though the model accounted for heterogeneous material, the application was still restricted to uniform cross-section. A comprehensive overview of models adopted for analysis of laminated beams and plates with particular attention towards vibration and wave propagation is summarized by Kapania and Raciti [8]. Kant et al. reported an analytical solution to the natural frequency analysis of composite and sandwich beam structure based on a higher-order refined theory [7] and dealt with dynamic response analyses [9]. Librescu developed refined beam modes accounting for non-classical effects with particular attention paid to aircraft structures [10].

The development of advanced models for structural dynamics based on beam theories is currently being

carried out by many researchers. Latest contributions focused on damage detection [11], spectral finite elements [12–14], layer-wise models [15, 16], and viscoelastic materials [17].

The inherent limitation in most of the aforementioned papers is the problem dependency of the theories. The current paper adopts a generalized 1D refined beam model, which maintains the generality regarding the geometric and material description of the problem. The refined beam models are developed within the framework of the CUF, a hierarchical formulation which offers a methodology to procure refined structural theories that account for variable kinematics description [18]. Originally developed for plates and shells [19], CUF enables one to select arbitrary choice of expansion function over the cross-section of the beam[20]. Therefore, any structural theory can be modeled without any changes to the fundamental formulation. CUF models, when used in conjunction with 1D finite element framework, enables to solve structural problems of any arbitrary geometries, material configuration and boundary conditions without any ad hoc assumptions. CUF models can detect shell-like and solid-like response for various types of analyses. Over the last decade, two main classes of 1D CUF models have been developed [3]. Taylor Expansion (TE) models are based on Taylor-like polynomial, where the order of the polynomial determines the beam theory order [20]. Classical beam models such as Euler-Bernoulli beam theory (EBBT) and Timoshenko Beam Theory (TBT) are obtained as special cases of TE models. Lagrange polynomials are utilized to expand displacement field over the cross-section in Lagrange Expansion (LE) models [21]. LE models allow representing every part of a multi-component structure via 1D finite element, leading to Component-Wise (CW) approach [22]. Various structural dynamics applications have been proposed in the last years, such as: free vibration [23], dynamic response [24], rotordynamics [25], exact dynamic stiffness elements [26], viscoelastic materials [27], and damaged structures [28]. The CW makes use of the 1D CUF models to deal with complex, multi-component structures via only 1D elements and has been used for various structural dynamics applications [29, 30].

The present paper exploits the 1D CUF models for wave propagation problems. In particular, this paper can be considered as a companion work of [31] in which TE models were used with implicit integration schemes. On the other hand, LE models and explicit integration schemes, and the CUF capabilities for wave propagation problems are assessed the first time here.

CUF models are employed to study the local deflection and stress histories of the structure. High-frequency finite element solutions for wave propagation problems are often associated with spurious oscillations, especially at the wavefront. The error in such simulation is cumulated due to numerical dispersions and

oscillations [32–35]. Much research has been dedicated towards eliminating spatial and temporal dispersion errors in wave propagation problems adopting higher-order finite elements [36], use of lumped mass matrices [37], employing modified spatial integration rules for mass and stiffness matrices [38], filtering spurious modes [39], and introducing numerical dissipations in the time integration scheme [34, 35, 40]. In the current framework, the spatial dispersion error is straightforwardly addressed by using higher-order formulations. The temporal dispersion is mitigated using a dissipative explicit scheme. The explicit scheme based on the bulk viscosity method (BVM) [40], in which a viscous pressure term is added to the dynamic equilibrium equation, is used in commercial software such as ABAQUS [41]. The Tchamwa-Wielgosz (TW) scheme eliminates oscillations introducing a damping parameter to the time integration equation [34]. In the current work, the stress wave propagation problem is solved using the TW scheme in conjunction with a lumped mass matrix. Due to the diagonal mass matrix, the time marching operations is limited to simple mathematical operation.

The paper is organized as follows: Section 2 presents a brief overview of the 1D CUF theory; then, the finite element formulation and time integration scheme adopted in the paper is discussed; the numerical results are presented in Section 3; finally, the concluding remarks are outlined in Section 4.

2 Variable Kinematics Beam Theories via CUF

The coordinate system adopted is illustrated in Fig. 1. The longitudinal axis of the beam coincides with the y-axis of the coordinate system ($0 \leq y \leq L$) and the cross-section Ω is overlayed on the x-z plane. The displacement vector is

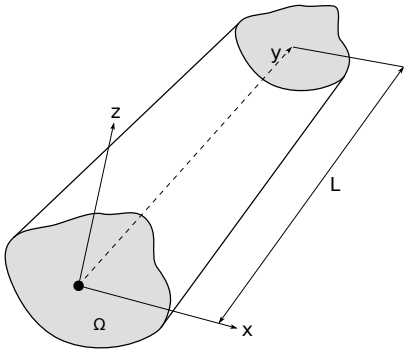

Figure 1: Coordinate system for the 1D beam model

$$\mathbf{u}(x, y, z) = \{u_x \; u_y \; u_z\}^T \tag{1}$$

The CUF expresses the displacement field as an expansion of generic cross-section functions, $F_\tau(x,z)$,

$$\mathbf{u}(x,y,z,t) = F_\tau(x,z)\mathbf{u}_\tau(y,t) \quad \tau = 1,2,....,M \tag{2}$$

Where $\mathbf{u}_\tau(y)$ contains the unknown, generalized, displacement variables. M stands for the number of terms in the cross-section expansion function F_τ. The class of 1D CUF model adopted is based on the choice of F_τ. Two classes of cross-section expansion functions are introduced within the context of this paper: (1) Taylor Expansions (TE) and (2) Lagrange Expansions (LE). TE 1D models are based on the polynomial expansions of the kind $x^i z^j$, as cross-section expansion function F_τ, where i and j are positive integers. For instance, a second-order TE 1D model ($N = 2$, $M = 6$) can be expressed as follows:

$$\begin{aligned} u_x &= u_{x1} + xu_{x2} + zu_{x3} + x^2u_{x4} + xzu_{x5} + z^2u_{x6} \\ u_y &= u_{y1} + xu_{y2} + zu_{y3} + x^2u_{y4} + xzu_{y5} + z^2u_{y6} \\ u_z &= u_{z1} + xu_{z2} + zu_{z3} + x^2u_{z4} + xzu_{z5} + z^2u_{z6} \end{aligned} \tag{3}$$

The order of the expansion (N) is arbitrary and defines the beam theory. A noteworthy feature of TE 1D model is that classical beam theories such as EBBT and TBT can be obtained as particular cases of first-order TE 1D model ($N = 1$).

LE 1D models are formulated using Lagrange polynomials as cross-section function F_τ. These expansion functions consist of purely displacement variables, whereas 1D TE models are characterized with displacements and N-order derivatives of the displacement. The cross-section is discretized into some LE elements. In this paper, L9 cross-section elements were used. The expansion functions for an L9 element are

$$\begin{aligned} F_\tau &= \frac{1}{4}\left(r^2 + rr_\tau\right)\left(s^2 + ss_\tau\right), \quad \tau = 1,2,5,7 \\ F_\tau &= \frac{1}{2}s_\tau^2\left(s^2 - ss_\tau)(1-r^2)\right) + \frac{1}{2}r_\tau^2\left(r^2 - rr_\tau\right)\left(1-s^2\right), \quad \tau = 2,4,6,8 \\ F_\tau &= \left(1-r^2\right)\left(1-s^2\right), \quad \tau = 9 \end{aligned} \tag{4}$$

where r and s range from -1 to $+1$ and r_τ and s_τ are the coordinates of the nine nodes. Therefore, a beam theory based on L9 has the following displacement field:

$$\begin{aligned} u_x &= F_1 u_{x_1} + F_2 u_{x_2} + ... + F_9 u_{x_9} \\ u_y &= F_1 u_{y_1} + F_2 u_{y_2} + ... + F_9 u_{y_9} \\ u_z &= F_1 u_{z_1} + F_2 u_{z_2} + ... + F_9 u_{z_9} \end{aligned} \tag{5}$$

where $u_{x_1}, ..., u_{x_9}$ represent the translational displacement component of each of the nine nodes in the L9 element.

2.1 Geometrical and constitutive laws

The stress, $\boldsymbol{\sigma}$, and strain, $\boldsymbol{\epsilon}$, are grouped as follows:

$$\boldsymbol{\sigma} = \{\sigma_{xx}\ \sigma_{yy}\ \sigma_{zz}\ \sigma_{xy}\ \sigma_{xz}\ \sigma_{yz}\}^T, \qquad \boldsymbol{\epsilon} = \{\epsilon_{xx}\ \epsilon_{yy}\ \epsilon_{zz}\ \epsilon_{xy}\ \epsilon_{xz}\ \epsilon_{yz}\}^T \tag{6}$$

With small strain assumptions, the linear strain-displacement relation is

$$\boldsymbol{\epsilon} = \mathbf{D}\,\mathbf{u} \tag{7}$$

where $\mathbf{D}$ is the linear differential operator on $\mathbf{u}$ and is

$$\mathbf{D} = \begin{bmatrix} \frac{\partial}{\partial x} & 0 & 0 \\ 0 & \frac{\partial}{\partial y} & 0 \\ 0 & 0 & \frac{\partial}{\partial z} \\ \frac{\partial}{\partial y} & \frac{\partial}{\partial x} & 0 \\ \frac{\partial}{\partial z} & 0 & \frac{\partial}{\partial x} \\ 0 & \frac{\partial}{\partial z} & \frac{\partial}{\partial y} \end{bmatrix} \tag{8}$$

For linear elastic material, stress can be related to strain as follows:

$$\boldsymbol{\sigma} = \mathbf{C}\boldsymbol{\epsilon} \tag{9}$$

where $\mathbf{C}$ is the 6×6 elastic material matrix. For the sake of brevity, the explicit expressions of C_{ij} are not given here, but can be found in [42].

2.2 Finite element formulation

Adopting the conventional FE approach to discretize the beam along its y-axis, the displacement vector $\mathbf{u}$ can be expressed as

$$\mathbf{u}(x, y, z) = F_\tau(x, z) N_i(y) \mathbf{u}_{\tau i}; \quad \tau = 1, ..., M; \quad i = 1, ..., p + 1 \tag{10}$$

Where N_i is the beam shape function of order p and $\mathbf{u}_{\tau i}$ is the nodal displacement vector,

$$\mathbf{u}_{\tau i} = \{u_{x_{\tau i}} \;\; u_{y_{\tau i}} \;\; u_{z_{\tau i}}\}^T \tag{11}$$

Three types of beam elements are adopted within the CUF framework, B2 (two nodes), B3 (three nodes) and B4 (four nodes), which represents linear, quadratic and cubic approximation respectively. Standard FE shape functions are used and not reported here for the sake of brevity, but can be found in [32]. It should be noted that the choice of expansion function of the cross-section and choice of the beam finite element remains independent. In this work, B4 elements are adopted. The principle of virtual displacement holds

$$\delta L_{int} = \delta L_{ext} - \delta L_{ine} \tag{12}$$

Where L_{int} stands for internal strain energy, L_{ext} stands for work done by the external loads, L_{ine} is the work due to inertial loading and δ stands for the virtual variation. The stiffness and mass matrices and loading vector are obtained via manipulation of Eqn. 12. The virtual variation of strain energy δL_{int} can be written as

$$\begin{aligned} \delta L_{int} &= \int_V \delta \boldsymbol{\epsilon}^T \boldsymbol{\sigma} dV \\ &= \delta \mathbf{u}_{sj}^T \mathbf{K}^{ij\tau s} \mathbf{u}_{\tau i} \end{aligned} \tag{13}$$

Where $\mathbf{K}^{ij\tau s}$ is the stiffness matrix in the form of the fundamental nucleus (FN). The virtual variation of the work done by internal loading can be expressed as

$$\begin{aligned} \delta L_{ine} &= \int_V \rho \delta \mathbf{u}^T \ddot{\mathbf{u}} dV \\ &= \delta \mathbf{u}_{sj}^T \mathbf{M}^{ij\tau s} \ddot{\mathbf{u}}_{\tau i} \end{aligned} \tag{14}$$

Where $\mathbf{M}^{ij\tau s}$ is the FN of the mass matrix. The derivation and components of the FE fundamental nucleus is not reported here for the sake of conciseness but can be found in [32]. It is important to emphasis the fact that no inherent assumptions about the approximation order has been made in formulating $\mathbf{K}^{ij\tau s}$ and $\mathbf{M}^{ij\tau s}$. Therefore, the formal expression of the FN remains the same, which in turn allows formulating any class of beam theories with the same numerical implementation. The damping matrix $\mathbf{C}$ is defined as a linear combination of stiffness matrix $\mathbf{K}$ and mass matrix $\mathbf{M}$ using Rayleigh damping constants. Due to the computational advantage, lumped mass matrix is employed for an explicit scheme. Diagonal mass matrix is obtained by using Gauss-Lobatto integration rule [38]. For all other cases, consistent matrices are obtained through Gauss integration rule.

The virtual variation of external work due to a generic concentrated load $\mathbf{P}$ acting on a point (x_p, y_p, z_p) can be expressed as

$$\begin{aligned} \delta L_{ext} &= \delta \mathbf{u}^T \mathbf{P} \\ &= F_s N_j \delta \mathbf{u}_{sj}^T \mathbf{P} \end{aligned} \tag{15}$$

where F_s and N_j are evaluated at (x_p, z_p) and y_p, respectively.

2.3 Direct time integration scheme

The equations of motion can be written as

$$\mathbf{M}\ddot{\mathbf{U}} + \mathbf{C}\dot{\mathbf{U}} + \mathbf{K}\mathbf{U} = \mathbf{R} \tag{16}$$

Where $\mathbf{M}$, $\mathbf{C}$ and $\mathbf{K}$ are the assembled global mass, damping and stiffness matrices respectively, which are obtained by expanding the CUF FNs and assembling them into global arrays. $\mathbf{U}$, $\dot{\mathbf{U}}$. and $\ddot{\mathbf{U}}$ are the vector of nodal displacements, velocities and accelerations, respectively. $\mathbf{R}$ is the vector of nodal

external load. In this paper, two classes of time integration schemes are adopted to solve the dynamic wave propagation problem: (1) Newmark-β scheme and (2) Tchamwa-Wielgosz scheme.

A. Newmark-β scheme

The implicit scheme based on Newmark β can described as [43]:

$$\mathbf{M}\ddot{\mathbf{U}}_{n+1} + \mathbf{C}\dot{\mathbf{U}}_{n+1} + \mathbf{K}\mathbf{U}_{n+1} = \mathbf{R}_{n+1} \tag{17}$$

Implicit methods are unconditionally stable but require factorization of the assembled global matrices to obtain the solution at every step.

B. Tchamwa-Wielgosz scheme

Explicit methods are quite popular in wave propagation analysis. When used in conjunction with diagonal lumped mass matrix, the computational operation at each time step reduces to basic mathematical operations. Being conditionally stable, the time step size has a considerable effect on stability and spurious oscillations in an explicit scheme. The explicit method based on the Tchamwa-Wielgosz (TW) scheme is implemented in the current framework [34]. The scheme can damp spurious oscillation more quickly. The TW scheme is controlled by a single parameter ϕ, which gives

$$\begin{aligned}
\mathbf{U}_{t+\Delta t} &= \mathbf{U}_t + \Delta t\dot{\mathbf{U}}_t + \phi\Delta t^2\ddot{\mathbf{U}}_t \\
\dot{\mathbf{U}}_{t+\Delta t} &= \dot{\mathbf{U}}_t + \frac{1}{2}\Delta\ddot{\mathbf{U}}_t \\
\ddot{\mathbf{U}}_{t+\Delta t} &= \mathbf{M}^{-1}\left[\mathbf{R}_{t+\Delta t} - \mathbf{C}\dot{\mathbf{U}}_{t+\Delta t} - \mathbf{K}\mathbf{U}_{t+\Delta t}\right]
\end{aligned} \tag{18}$$

Where Δt is the time increment. The parameter ϕ controls the damping efficiency of the scheme. The critical time step size is defined as

$$\Delta t_{cr} = \frac{2}{\omega_n} \tag{19}$$

Where ω_n is the largest eigen frequency of the assembled system. A power iteration method is used to compute the ω_n [44].

3 Results

The numerical results deal with typical wave propagation and traveling load problems in isotropic, composite and thin-walled structures. Comparisons with analytical models or 3D FE are provided.

3.1 1D stress wave propagation

A classic, 1D wave propagation problem was first considered to validate the numerical framework implemented and assess the accuracy and stability of the present 1D formulation against analytical and 3D FE. Idealizing the problem to A 1D case is a commonly adopted technique in literature to validate new numerical frameworks [34, 35]. Due to the availability of analytical solutions, it also serves as a good benchmark for evaluating the capabilities of the proposed beam finite element model.

The beam is isotropic material with the Young modulus (E) of 207 GPa and density (ρ) of 7800 kgm^{-3}. Poisson's ratio was taken as zero. The geometry and boundary conditions of the problem are illustrated in Fig. 2. The length of the beam (L) is 5.0 m with a square cross-section of side ($w = h$) 0.2 m. The beam is clamped at one end, and an impact pressure load was applied at the free end with a time-histogram as illustrated in Fig. 3. Since it is a 1D wave propagation problem, the lateral edges of the beam were

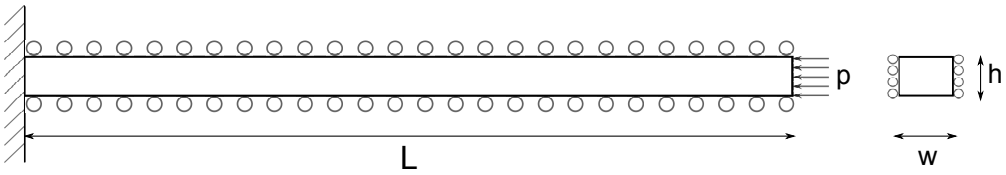

Figure 2: Geometry for the 1D stress wave propagation problem

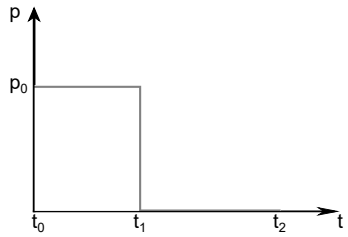

Figure 3: Load time history for the 1D stress wave propagation problem

constrained such as $u_x = u_z = 0$. The pulse load $p_0 = 0.1$ MPa was applied for a duration from 0 (t_0) - 0.19 (t_1) ms. The governing wave equation for the 1D wave propagation problem is given by

$$\frac{\partial^2 u}{\partial y^2} = \frac{1}{c_0^2}\frac{\partial^2 u}{\partial t^2} \tag{20}$$

where c_0 is the wave speed of the material with $c_0 = \sqrt{E/\rho}$. The method of d'Alembert provides the solution to the 1D wave equation,

$$u(y,t) = f(y - c_0\, t) + g(y + c_0\, t) \tag{21}$$

where f and g are arbitrary functions representing right-traveling and left-traveling waves, respectively [45].

The beam was discretized using B4 elements and the cross-section was modeled using 1 L9 element. The problem was analyzed for a duration of 1.2 ms. A lumped mass matrix with the explicit Tchamma-Wielgosz scheme was utilized for time integration. The damping parameter ϕ was set to 1.013. Artificial damping was introduced into the system through proportional stiffness damping. A similar model was developed in ABAQUS using 3D brick elements and BVM based explicit scheme for time integration [41]. Total degrees of freedom for CUF-LE and ABAQUS models were 1890 (70 B4 elements) and 3012 (250 brick elements), respectively.

The stress and velocity distribution along the beam at various instants are reported in Fig. 4. The solution is compared against analytical and ABAQUS results. Stress wave propagation contours at various instants are illustrated in Fig. 5. A convergence study was undertaken to study the effect of mesh discretization with a various number of elements along the axis (see Fig. 6). The results suggest that

1. The present formulation can model the wave propagation with good accuracy.
2. The spurious oscillations were successfully mitigated, even at the reflected wave front.
3. The dispersion error was almost nullified with 70 elements along the beam axis.
4. CUF-LE model required only 70 elements as compared to ABAQUS with 250 brick elements, for producing dispersion error free results.

3.2 Traveling load

In the following section, beam structures under traveling loading conditions are investigated. The traveling wave is described as a step profile of pressure which travels along the axis of the beam with constant velocity (v_y) as illustrated in Fig. 7. Two structures were investigated with different loading conditions. An implicit time integration scheme was used to obtain the solution.

(a) Propagating wave

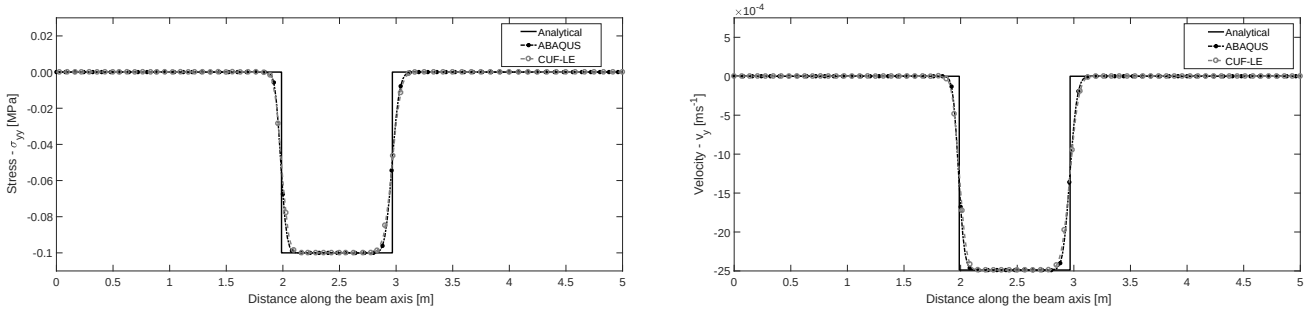

(b) At boundary - superposition of waves

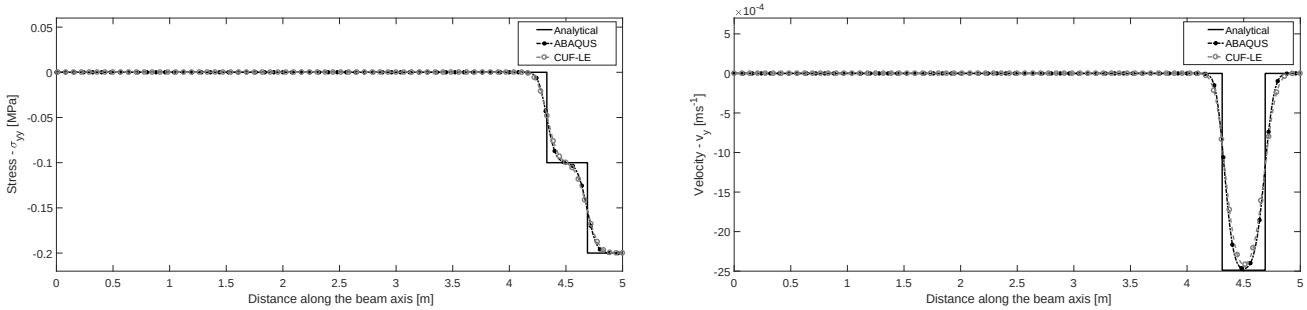

(c) Reflecting wave

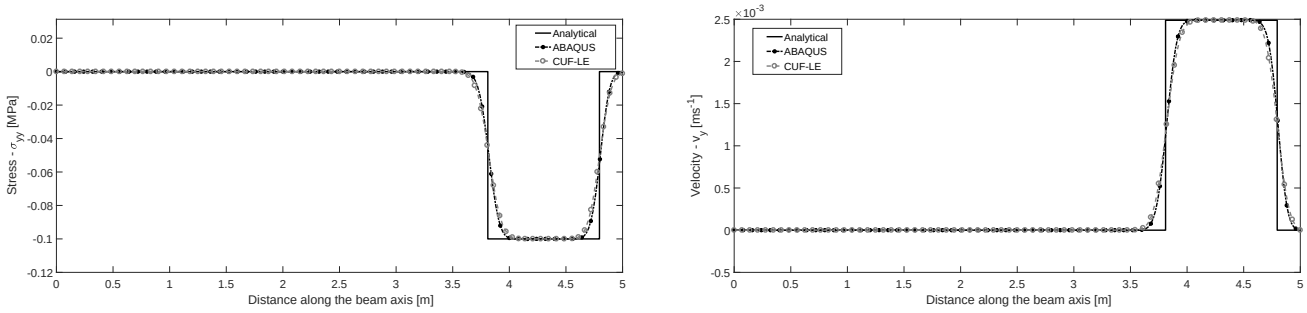

(a) Stress distribution **(b)** Velocity distribution

Figure 4: Stress and velocity distributions along the beam at (a) $t = 0.58$ ms (b) $t = 1.01$ ms and (c) $t = 1.2$ ms using 70 B4-elements for the 1D stress wave problem

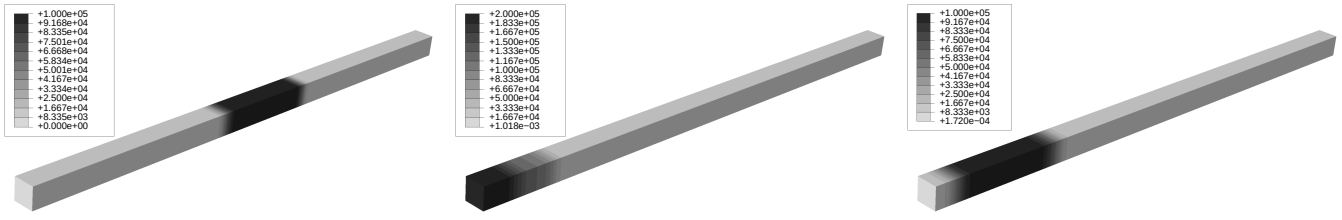

(a) **(b)** **(c)**

Figure 5: Stress (σ_{yy}) wave propagation in beam at (a) 0.58 ms (b) 1.03 ms and (c) 1.2 ms for the 1D stress wave problem

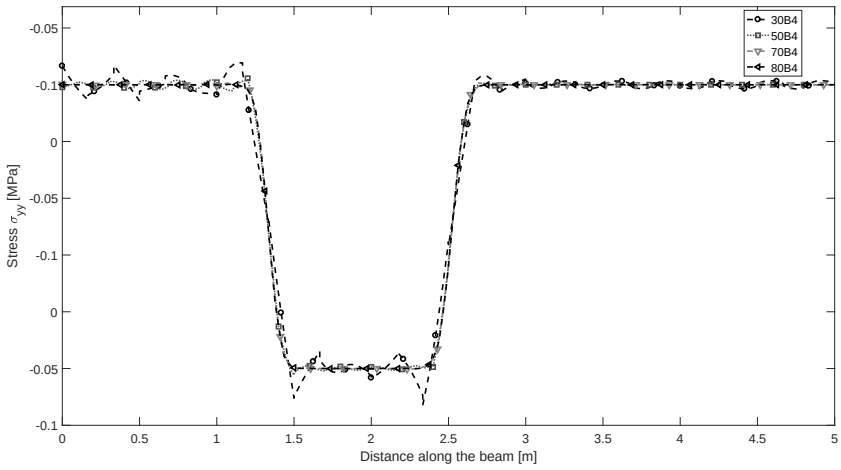

Figure 6: Convergence study for the 1D stress wave propagation problem

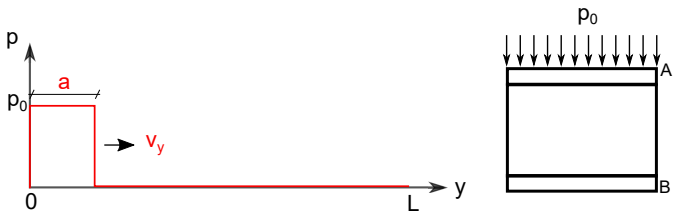

Figure 7: Pressure step profile traveling along the beam axis with velocity v_y

A. Sandwich structure

A clamped-clamped composite sandwich beam structure is investigated. The sandwich consists of an isotropic foam with composite plates at the bottom and top, see Fig. 8. The material properties of the individual composite sandwich components are listed in Table 1. The wave is described as a step profile

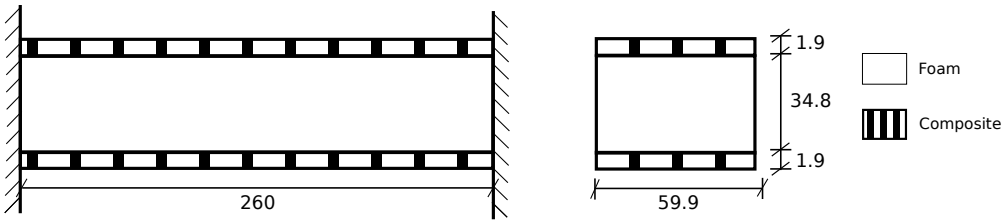

Figure 8: Geometry of the composite sandwich beam (all dimensions in mm)

Table 1: Material properties of the composite sandwich beam

	E_{11} (GPa)	E_{22}/E_{33} (GPa)	ν_{12}/ν_{13} -	ν_{23} -	G_{12}/G_{13} (GPa)	G_{23} (GPa)	ρ (Kgm^{-3})
Composite	276	15	0.279	0.3	12	5.02	1500
Foam		2.487		0.35		1.91	60

Table 2: Displacement $[u_z]$ at the mid-span of the beam at point A at 6.5 ms for the composite sandwich beam problem

	DOFs -	u_z^{max} (10^{-4} m)	u_x^{max} (10^{-6} m)
TE			
EBBT	93	0.311	0.473
TBT	155	0.313	0.484
N=1	279	0.313	0.484
N=2	558	0.320	0.695
N=3	930	3.173	1.257
N=4	1,395	3.246	1.781
N=5	1,953	3.317	8.699
N=6	2,604	3.342	9.357
N=7	3,348	3.742	9.525
N=8	4,185	3.759	10.080
N=9	5,115	3.854	10.260
N=10	6,138	3.831	9.740
N=11	7,254	3.856	9.664
N=12	8,463	3.861	9.590
N=13	9,765	3.946	9.594
LE			
3L9	1,953	4.085	7.280
6L9	3,255	4.087	9.435

of pressure which travels along the beam axis with constant velocity (v_y) of 19 ms^{-1} and pressure of $-0.48MPa$. The extension of the step profile is described by the length $a = L/20$ (see Fig. 7). The structure was discretized as a beam with 10 B4 elements since such mesh provided good convergence for this loading case. The cross-section of the beam was modeled using TE and LE as depicted in Fig. 9. The solution was obtained for a duration of 13 ms. The displacements were evaluated at point A (see

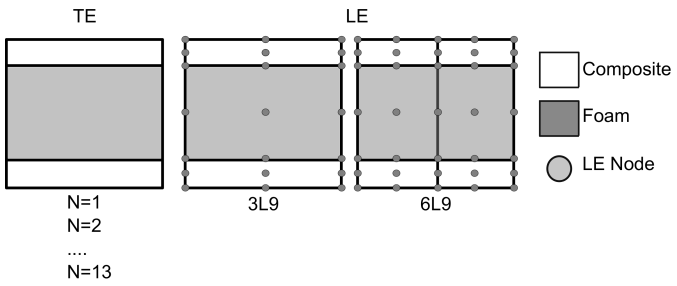

Figure 9: Cross-section configurations for the sandwich beam

Fig. 7) at $t = 6.5$ ms for various beam configurations is tabulated, see Table 2. Figure 10 illustrates the displacement $[u_z]$ profile along the beam axis at point A for various beam configurations at $t = 6.5$ ms. The time history of the displacement $[u_z]$ at point A is plotted in Fig. 11. The 3D configuration of the sandwich beam at various instants is illustrated in Fig. 12. The normal stress distribution along the edge

AB of the cross-section (see Fig. 7) at the mid-span of the beam at $t = 6.5$ ms is depicted in Fig. 13. The results suggest the following:

1. The travelling pressure causes severe local effects due to the presence of the soft core.
2. Classical models, such as EBBT and TBT, and low order TE models clearly fail to capture the displacement field (see Table 2). In fact, such models cannot predict cross-sectional distortions.
3. TE model of order N = 13 and LE-6L9 provide similar displacement and stress fields, even though they differ greatly regarding the degrees of freedom required to model the problem.
4. No considerable difference in stress and displacement fields was observed for LE-3L9 and LE-6L9.
5. LE models are more efficient than TE model because of their capability to capture local displacement field via local refinements.

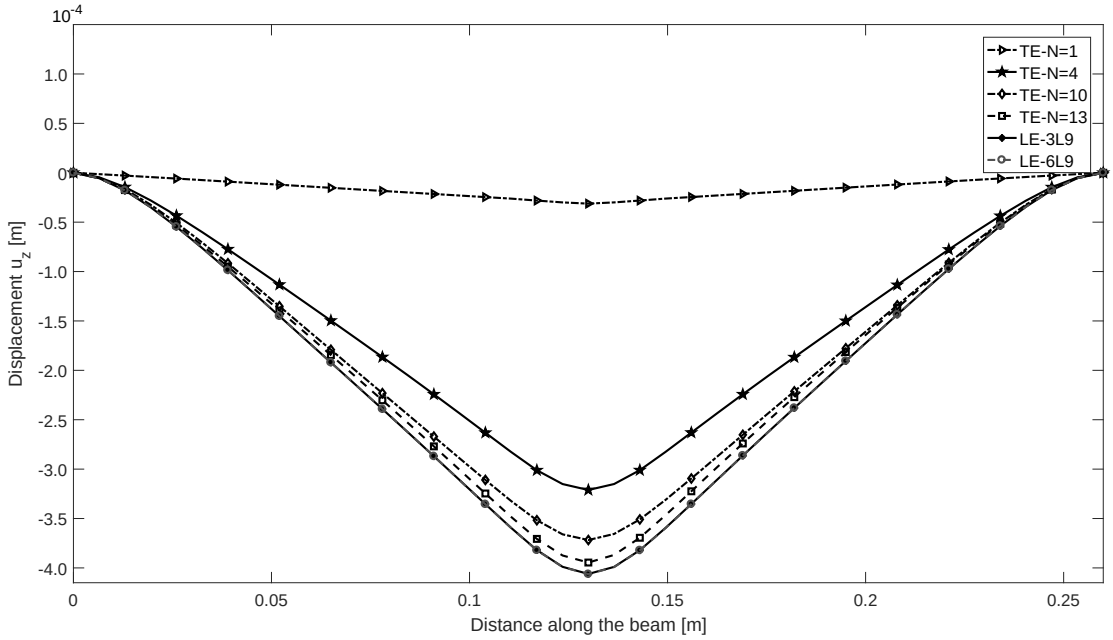

Figure 10: Displacement profile $[u_z]$ along the beam axis at point A (see Fig. 7) for various beam configurations at $t = 6.5$ ms, composite sandwich beam problem

B. Three-layered annular cylinder

A three-layered, thin-walled cylinder is investigated. The problem statement is based on the works of Varello et al. [46]. The geometry and layer configuration for the cross-section of the structure are

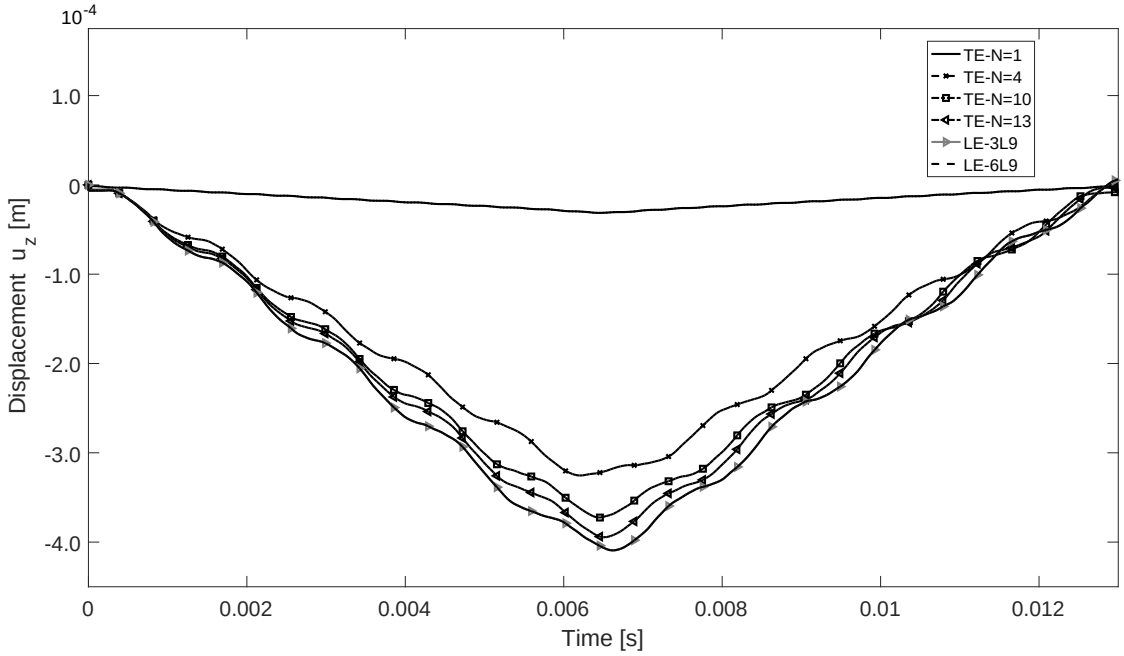

Figure 11: Time history of displacement $[u_z]$ at point A (see Fig. 7) for various beam configurations, composite sandwich beam problem

illustrated in Fig. 16a. The external diameter (d_e) and internal diameter (d_i) of the cylinder are 100 mm and 94 mm, respectively. The thickness of each layer amounts to 1 mm. The material properties of the layers are summarized in Table 3. The length of the cylinder (L) is 500 mm. The structure is subjected to clamped boundary conditions at the ends, $y = 0$ and $y = L$. The structure was subjected to two

Table 3: Material properties of different layers in three-layered annular cylinder problem

Property	Unit	Layer 1	Layer 2	Layer 3
Young's Modulus (E)	GPa	69	30	15
Poisson's ratio (ν)	-	0.33	0.33	0.33
Density (ρ)	kgm^{-3}	2700	2000	1800

loads,

1. A uniform pressure $p_1 = 0.148$ MPa was applied on the internal surface of the cylinder (upper surface of layer 1, $r = d_i/2$; $90^o \leq \theta \leq 270^0$; $0 \leq y \leq L$, see Fig. 16b).

2. A traveling load of step length $a = L/10 = 50$ mm and a pressure value $p_2 = -1.727$ MPa with a constant velocity $v_y = 90$ ms^{-1} (see Fig. 7) was applied on the internal surface of the cylinder (upper surface of layer 1, $r = d_i/2$; $90^o \leq \theta \leq 270^0$, see Fig. 16b).

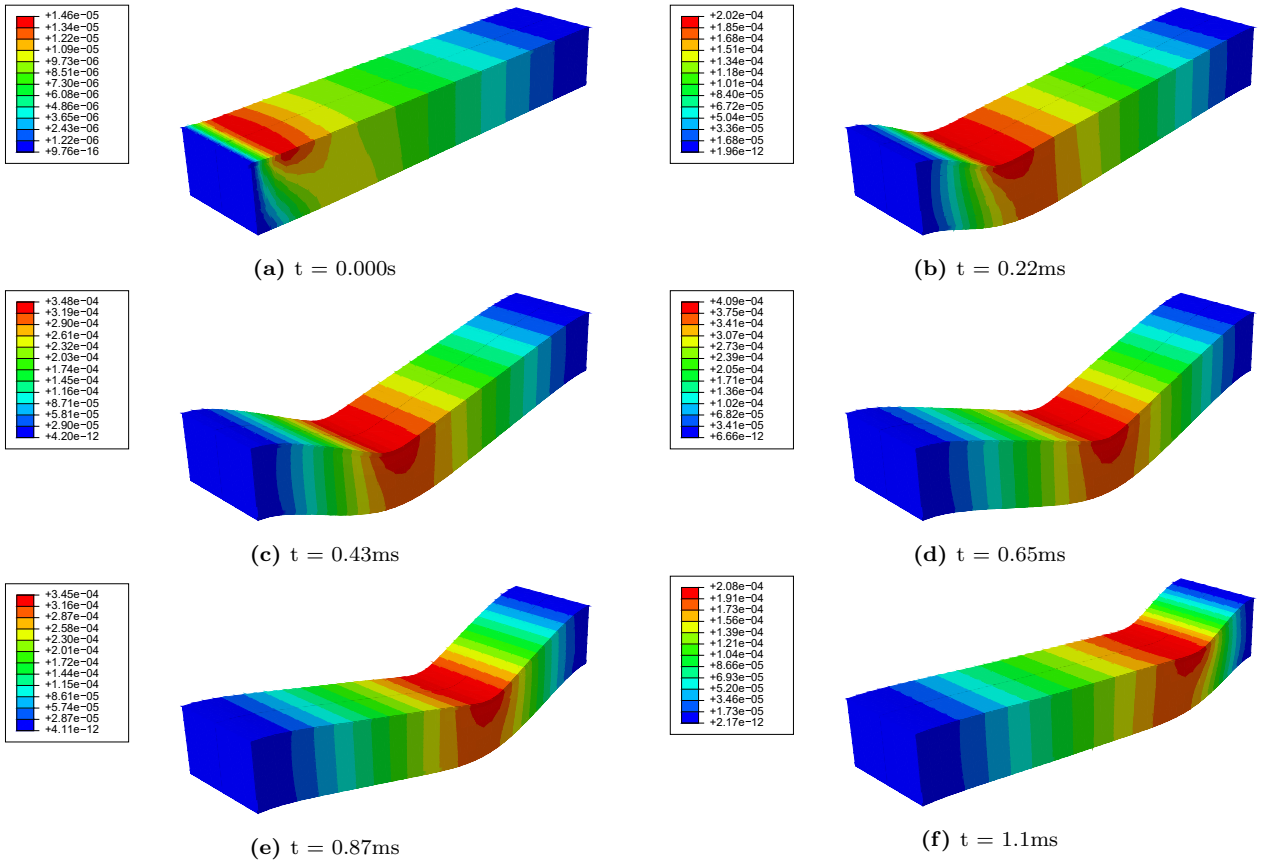

(a) t = 0.000s

(b) t = 0.22ms

(c) t = 0.43ms

(d) t = 0.65ms

(e) t = 0.87ms

(f) t = 1.1ms

Figure 12: 3D deformation configuration and resultant displacement (m) at various time steps for wave propagation in sandwich (LE-6L9 model) for the composite sandwich beam problem

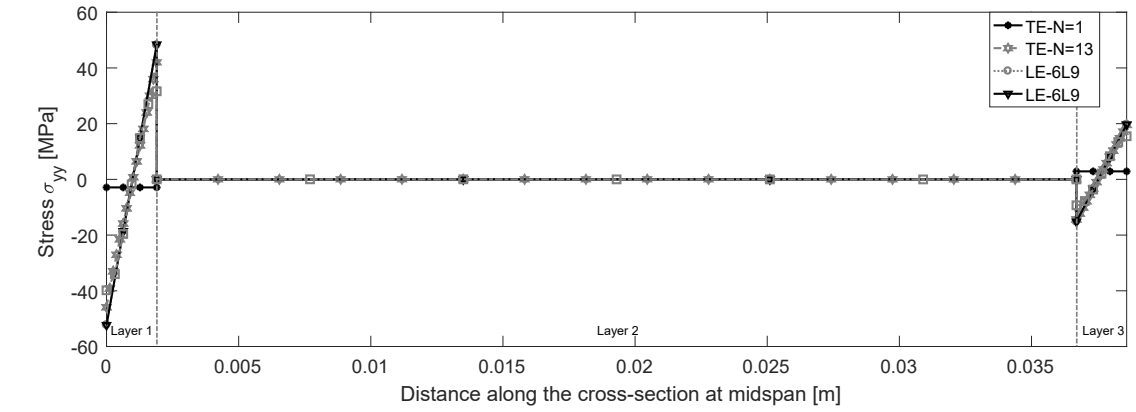

(a)

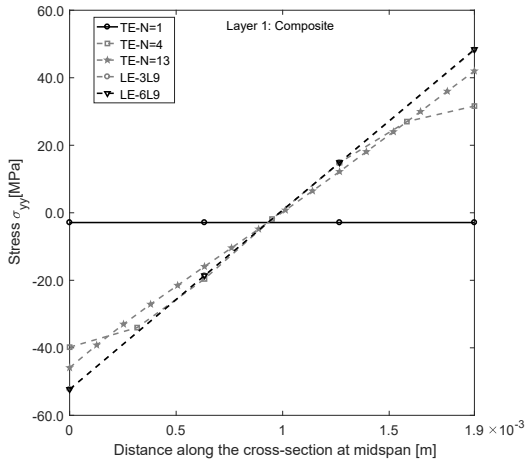

(b)

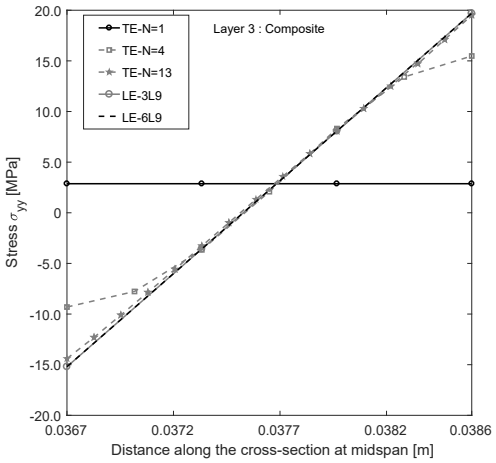

(c)

Figure 13: Normal stress distribution σ_{yy} (a) along the edge of the cross-section AB, (b) layer 1, and (c) layer 3 (see Fig. 7) at mid-span of the beam at $t = 6.5$ ms for the composite sandwich beam problem

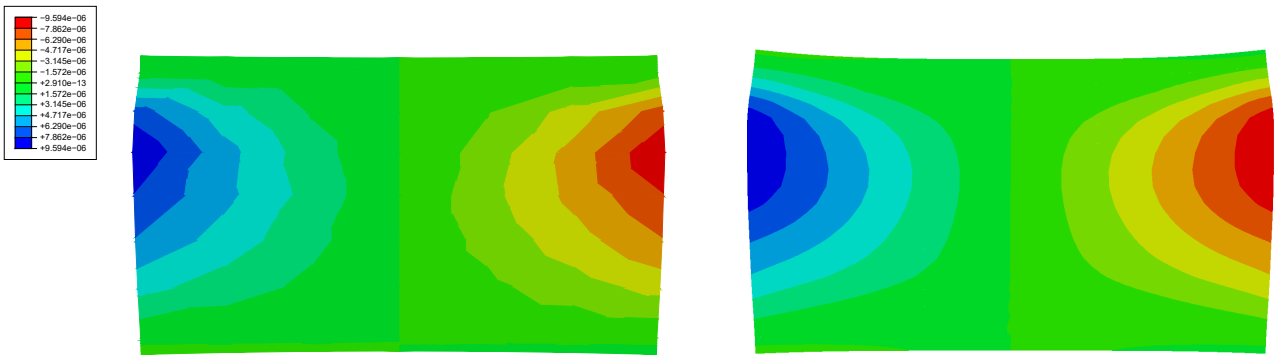

(a) LE-6L9

(b) TE-N=13

Figure 14: Cross-section displacement field u_x (m) at mid-span of the beam at $t = 6.5$ ms for the composite sandwich beam problem

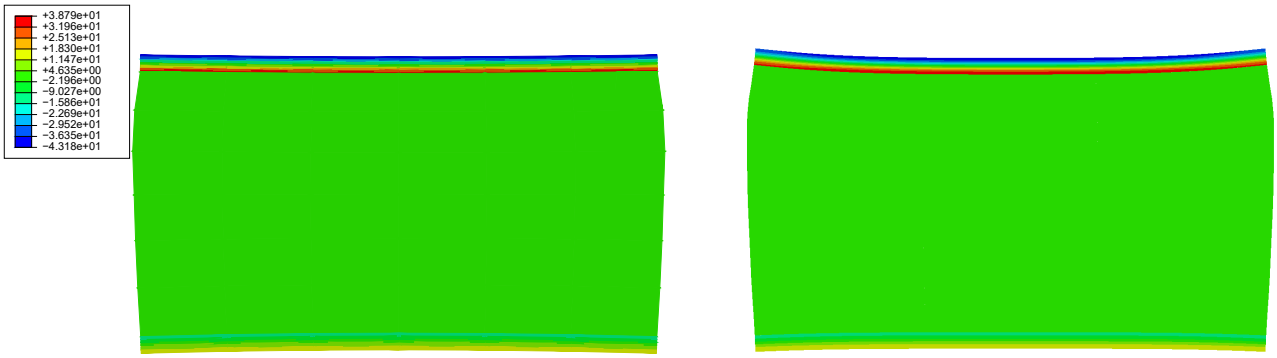

(a) LE-6L9 **(b)** TE-N=13

Figure 15: Stress field σ_{yy} (MPa) at mid-span of the beam at $t = 6.5$ ms for the composite sandwich beam problem

(a) Geometry and layer configuration **(b)** Loading condition and points for evaluation

Figure 16: Details of the cross-section for three-layered annular cylinder beam

The beam was discretized using 10 B4 elements. As depicted in Fig. 17, TE models up to order N = 8 and two LE models (72L9 and 126 L9) were used to model the cross-section of the beam. The solution was obtained for a duration of 5 ms with the implicit scheme.

Table 4 shows the maximum displacements at 2.5 ms and the related angle along the cross-section. The 3D deformation of the beam structure at various instants is depicted in Fig. 18. Deformed configurations at the mid-span of the beam at various time instants are illustrated in Fig. 20. The displacement time history of point C (see Fig.16b) in the mid-span of the beam is depicted in Fig. 19. Normal stress distributions along the edge AB of the cross-section (see Fig. 16b) at the mid-span of the beam at t = 2.5 ms sre depicted in Fig. 21. The results suggest the following:

1. As for the previous case, loads cause severe cross-sectional distortions.

2. The 1D CUF models can capture local deformation state.

3. In this case, LE models are computationally more cumbersome than TE ones.

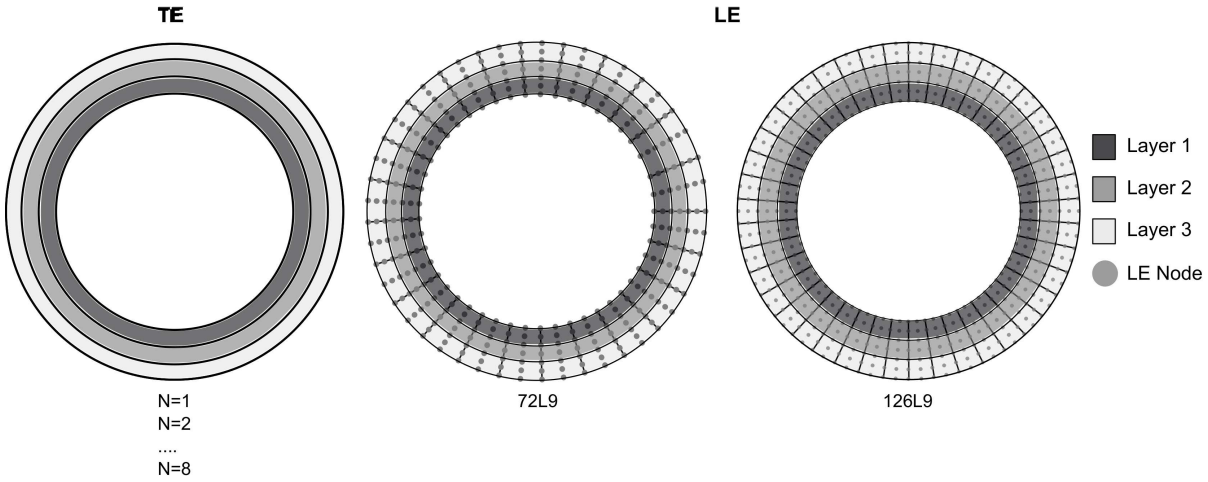

Figure 17: TE and LE cross-section models for the annular cylinder problem

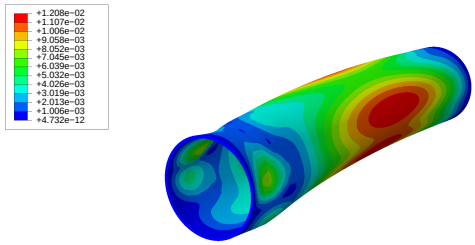

(a) t = 0.0 ms

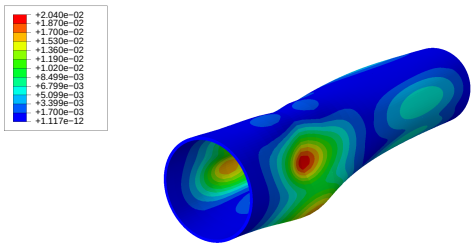

(b) t = 1.0 ms

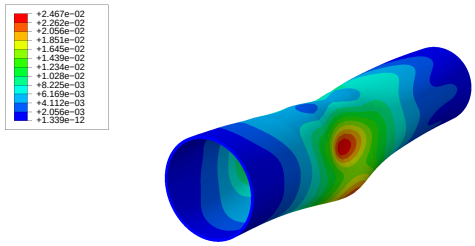

(c) t = 2.0 ms

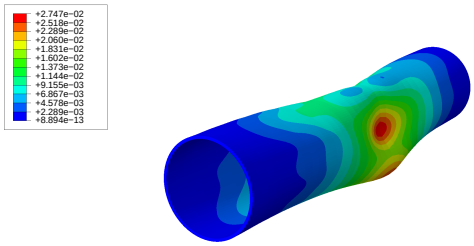

(d) t = 3.0 ms

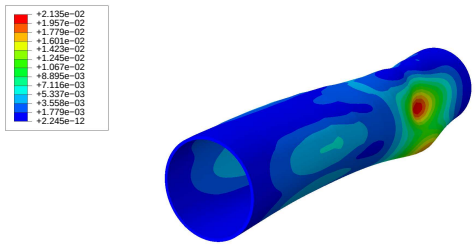

(e) t = 4.0 ms

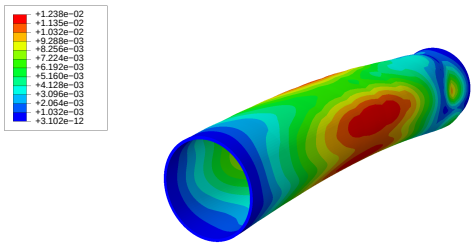

(f) t = 5.0 ms

Figure 18: 3D deformed configurations and resultant displacement (m) at various time steps for for the annular cylinder problem, 126 L9

Table 4: Displacements at the mid-span of the beam at 2.5 ms for the annular cylinder problem

	DOF	u_x^{max}	u_y^{max}	u_z^{max}	θ_{max}
	-	$(10^{-4}\,m)$	$(10^{-4}\,m)$	$(10^{-4}\,m)$	$(^\circ)$
TE					
EBBT	93	0.038	0.017	0.916	90
TBT	155	0.038	0.017	0.916	90
N=1	279	0.038	0.017	0.916	90
N=2	558	0.056	0.020	1.097	90
N=3	930	0.215	0.020	1.693	113
N=4	1,395	0.502	0.020	1.730	120
N=5	1,953	0.850	0.020	1.915	117
N=6	2,604	1.064	0.020	2.016	117
N=7	3,348	1.145	0.020	2.049	117
N=8	4,185	1.403	0.021	2.228	117
LE					
72L9	31,248	1.390	0.021	2.189	115
126L9	45,570	1.440	0.021	2.213	117

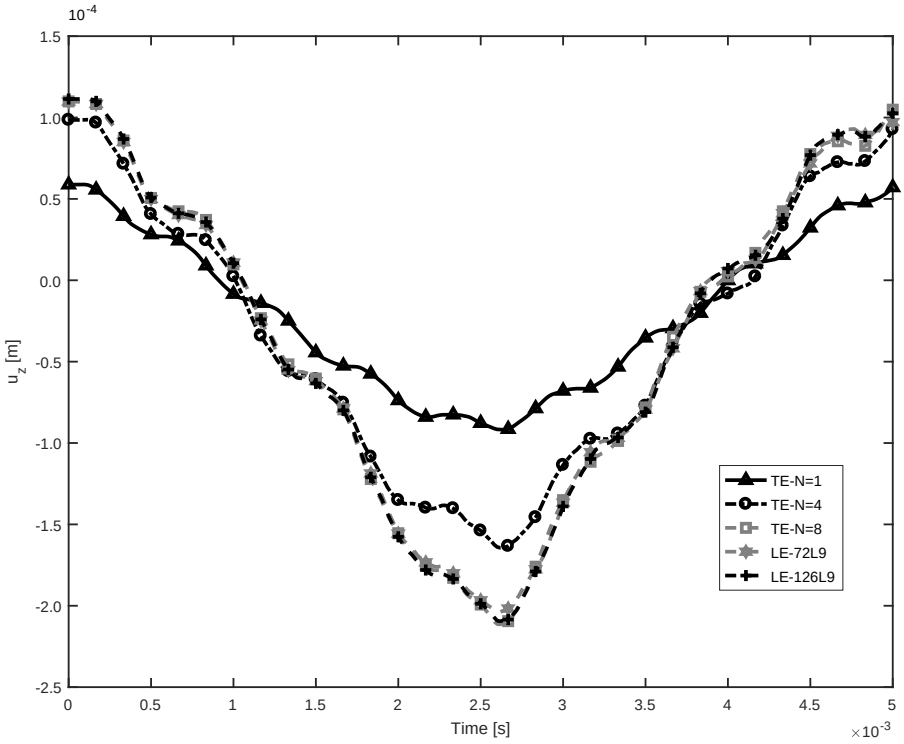

Figure 19: Displacement u_z at point C (see Fig. 16b) at the mid-span of the beam for the annular cylinder problem

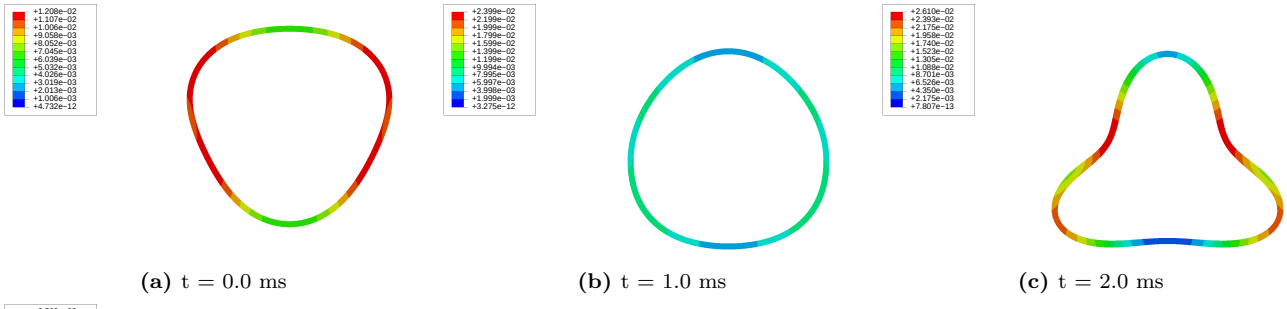

(a) t = 0.0 ms **(b)** t = 1.0 ms **(c)** t = 2.0 ms

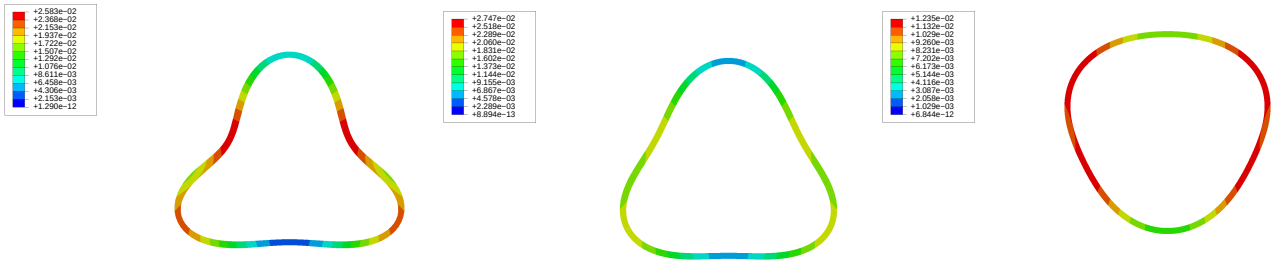

(d) t = 3.0 ms **(e)** t = 4.0 ms **(f)** t = 5.0 ms

Figure 20: Deformation configuration and resultant displacement (m) of the cross-section at the mid-span of the beam at various time steps for the annular cylinder problem, 126 L9

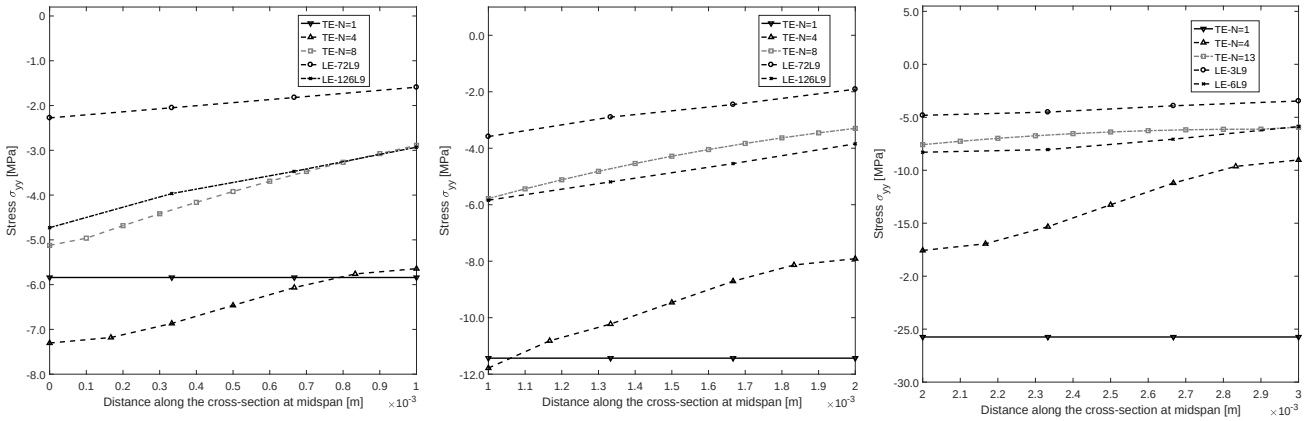

(a) Layer 1 **(b)** Layer 2 **(c)** Layer 3

Figure 21: Normal stress distribution σ_{yy} along the length AB of the cross-section (see Fig. 16b) at the mid-span of the beam at 2.5 ms for the annular cylinder problem

4 Conclusion

The paper investigates wave propagation characteristics of structures via 1D finite element models based of the Carrera Unified Formulation (CUF). Two classes of beam theories have been employed within the framework of CUF, namely Taylor Expansion (TE) models, and Lagrange Expansion (LE) models. The versatility of the proposed framework is demonstrated by presenting results for compact isotropic, sandwich structures, and thin-walled layered cylinder using the same formal implementation. Following conclusions can be drawn:

1. As well known, classical beam models tends to provide inaccurate results as soon as local effects are concerned.

2. CUF models can detect local, 3D-like, cross-sectional effects with high accuracy.

3. Spurious oscillations were successfully mitigated with 70 beam elements. Comparable results were obtained in ABAQUS with 250 brick elements.

4. LE models are particularly efficient to deal with structures with diverse material distributions as LE models can assign material characteristics locally via the cross-section Lagrange elements.

5. TE models perform better for thin-walled structures with reduced material heterogeneity.

Future work could deal with the extension to lamb waves problems for damage detection.

5 Acknowledgment

This research work has been carried out within the project FULLCOMP (FULLy analysis, design, manufacturing, and health monitoring of COMPosite structures), funded by the European Union Horizon 2020 Research and Innovation program under the Marie Skłodowska-Curie grant agreement No. 642121.

References

[1] Euler. De curvis elasticis. *Bousquest, Geneva*, 1744.

[2] S. P. Timoshenko. On the correction for shear of the differential equation for transverse vibration of prismatic bars. *Philosophical Magazine Series*, 41(6):744–746, 1921.

[3] E. Carrera, A. Pagani, M. Petrolo, and E. Zappino. Recent developments on refined theories for beams with applications. *Mechanical Engineering Reviews*, 2(2):1–30, 2015. doi: 10.1299/mer.14-00298.

[4] L. C. Bank and C.-H. Kao. Dynamic response of thin-walled composite material Timoshenko beams. *Journal of Energy Resources Technology*, 112, 1990.

[5] H. Murakami and J. Yamakawa. Development of one-dimensional models for elastic waves in heterogeneous beams. *Journal of Applied Mechanics*, 67:671–684, 1998.

[6] F. Gruttmann and W. Wagner. Shear correction factors in Timoshenko's beam theory for arbitrary shaped cross-sections. *Computational Mechanics*, 27:199207, 2001.

[7] T. Kant, S. R. Marur, and G. S. Rao. Analytical solution to the dynamic analysis of laminated beams using higher order refined theory. *Composite Structures*, 40(1):1–9, 1997.

[8] R. K. Kapania and S. Raciti. Recent advances in analysis of laminated beams and plates, part II: Vibrations and wave propagation. *AIAA Journal*, 27:935–946, 1989.

[9] S.R. Marur and T. Kant. On the performance of higher order theories for transient dynamic analysis of sandwich and composite beams. *Computers and Structures*, 65(5):741–759, 1997.

[10] L. Librescu and S. Na. Dynamic response of cantilevered thin-walled beams to blast and sonic-boom loadings. *Shock and Vibration*, 5(1):23–33, 1998.

[11] J. Metsebo, B.R. Nana Nbendjo, and P. Woafo. Dynamic responses of a hinged-hinged Timoshenko beam with or without a damage subject to blast loading. *Mechanics Research Communications*, 71:38–43, 2016.

[12] M. Mitra and S. Gopalakrishnan. Wavelet based spectral finite element for analysis of coupled wave propagation in higher order composite beams. *Composite Structures*, 73(3):263–277, 2006.

[13] N. Nanda, S. Kapuria, and S. Gopalakrishnan. Spectral finite element based on an efficient layerwise theory for wave propagation analysis of composite and sandwich beams. *Journal of Sound and Vibration*, 333(14):3120–3137, 2014.

[14] N. Nanda and S. Kapuria. Spectral finite element for wave propagation analysis of laminated composite curved beams using classical and first order shear deformation theories. *Composite Structures*, 132:310–320, 2015.

[15] A. Treviso, D. Mundo, and M. Tournour. A C^0-continuous RZT beam element for the damped response of laminated structures. *Composite Structures*, 131:987–994, 2015.

[16] M.A.R. Loja, J.I. Barbosa, and C.M. Mota Soares. Dynamic behaviour of soft core sandwich beam structures using kriging-based layerwise models. *Composite Structures*, 134:883–894, 2015.

[17] H. Arvin. Frequency response analysis of higher order composite sandwich beams with viscoelastic core. *Transactions of Mechanical Engineering*, 38(M1):143–155, 2014.

[18] Carrera E., Cinefra M., Petrolo M., and Zappino E. *Finite Element Analysis of Structures through Unified Formulation*. John Wiley and Sons, Ltd, 2014.

[19] E. Carrera. Theories and finite elements for multilayered plates and shells: A unified compact formulation with numerical assessment and benchmarking. *Archives of Computational Methods in Engineering*, 10:215–296, 2003.

[20] Carrera E., Petrolo M., and Giunta G. *Beam Structures: Classical and Advanced Theories*. John Wiley and Sons, Ltd, 2014.

[21] E. Carrera and M. Petrolo. Refined beam elements with only displacement variables and plate/shell capabilities. *Meccanica*, 47:537–556, 2011.

[22] E. Carrera, Maiarú M., and M. Petrolo. Component-wise analysis of laminated anisotropic composites. *International Journal of Solids and Structures*, 49:1839–1851, 2012.

[23] E. Carrera, F. Miglioretti, and M. Petrolo. Computations and evaluations of higher-order theories for free vibration analysis of beams. *Journal of Sound and Vibration*, 331:4269–4284, 2012.

[24] A. Pagani, M. Petrolo, G. Colonna, and E. Carrera. Dynamic response of aerospace structures by means of refined beam theories. *Aerospace Science and Technology*, 46:360–373, 2015. doi: 10.1016/j.ast.2015.08.005.

[25] E. Carrera and M. Filippi. Variable kinematic one-dimensional finite elements for the analysis of rotors made of composite materials. *Journal of Engineering for Gas Turbines and Power*, 136(9), 2014. doi: 10.1115/1.4027192.

[26] A. Pagani, E. Carrera, , J. R. Banerjee, P.H. Cabral, G. Caprio, and A. Prado. Free vibration analysis of composite plates by higher-order 1D dynamic stiffness elements and experiments. *Composite Structures*, 118:654–663, 2014. doi: 10.1016/j.compstruct.2014.08.020.

[27] M. Filippi, E. Carrera, and A.M. Regalli. Layer-wise analyses of compact and thin-walled beams made of viscoelastic materials. *Journal of Vibration and Acoustics*, 138(6), 2016. doi: 10.1115/1.4034023.

[28] E. Carrera, A. Pagani, and M. Petrolo. Free vibrations of damaged aircraft structures by component-wise analysis. *AIAA Journal*, 50(10):3091–3106, 2016. doi: 10.2514/1.J054640.

[29] E. Carrera, A. Pagani, and M. Petrolo. Component-wise method applied to vibration of wing structures. *Journal of Applied Mechanics*, 80(4), 2013. doi:10.1115/1.4007849.

[30] E. Carrera and A. Pagani. Accurate response of wing structures to free-vibration, load factors, and nonstructural masses. *AIAA Journal*, 54(1):227–241, 2016. doi: 10.2514/1.J054164.

[31] E. Carrera and A. Varello. Dynamic response of thin-walled structures by variable kinematic one-dimensional models. *Journal of Sound and Vibration*, 331(24):5268–5282, 2012. doi: 10.1016/j.jsv.2012.07.006.

[32] K.J. Bathe. *Finite Element Procedures*. Prentice-Hall, Inc, USA, 1996.

[33] K. J. Bathe and E.L. Wilson. Stability and accuracy analysis of direct integration methods. *Earthquake Engineering and Structural Dynamics*, 1:283–291, 1973.

[34] L. Maheo, V. Grolleau, and G. Rio. Numerical damping of spurious oscillations: A comparison between the bulk viscosity method and the explicit dissipative tchamwa-wielgosz scheme. *Computational Mechanics*, 51:109–128, 2013.

[35] G. Noh, S. Ham, and K. J. Bathe. Performance of an implicit time integration scheme in the analysis of wave propagations. *Computers and Structures*, 123:93–105, 2013.

[36] Y. Mirbagheri, H. Nahvi, J. Parvizian, and A. Düster. Reducing spurious oscillations in discontinuous wave propagation simulation using high-order finite elements. *Computers and Mathematics with Applications*, 70:1640–1658, 2015.

[37] S. Wu. Lumped mass matrix in explicit finite element method for transient dynamics of elasticity. *Computer Methods in Applied Mechanics and Engineering*, 195:5983–5994, 2006.

[38] M. Guddati and B. Yue. Modified integration rules for reducing dispersion error in finite element methods. *Computer Methods in Applied Mechanics and Engineering*, 193:275–287, 2004.

[39] N. Homes and T. Belytschko. Postprocessing of finite element transient response calculations by digital filters. *Computers and Structures*, 6:211–216, 1976.

[40] D. J. Benson. Computational methods in Lagrangian and Eulerian hydrocodes. *Computer Methods in Applied Mechanics and Engineering*, 99:235–394, 1992.

[41] *ABAQUS 6.14 Documentation.*

[42] J.N. Reddy. *Mechanics of laminated composite plates and shells. Theory and Analysis.* CRC Press, 2^{nd} edition, 2004.

[43] N.M. Newmark. A method of computation for structural dynamics. *ASCE Journal of the Engineering Mechanics*, (85):67–94, 1959.

[44] Mises R. V. and H. Pollaczek-Geiringer. Praktische verfahren der gleichungsauflsung. *Journal of Applied Mathematics and Mechanics / Zeitschrift fr Angewandte Mathematik und Mechanik*, 9(2):152–164, 1929.

[45] K. F. Graff. *Wave Motion in Elastic Solids.* Dover Publications, Inc, USA, 1975.

[46] A. Varello and E. Carrera. Static and dynamic analysis of a thin-walled layered cylinder by refined 1D theories. In *10th World Congress on Computational Mechanics, São Paulo, Brazil*, July 2012.